

Analysis of Plasma Edge Turbulence with Statistically Robust Linear and Non-Linear Wavelet Analysis Techniques

B.Ph. van Milligen, C. Hidalgo, E. Sánchez,
M.A. Pedrosa, R. Balbín and I. García-Cortés
Asociación Euratom-CIEMAT, Madrid, Spain

Abstract

For a detailed analysis of turbulence, adequate analysis tools are required. Two general properties of turbulence make the application of standard analysis tools (spectral analysis) difficult: (1) intermittency, which causes the characteristics of turbulence to change on a relatively short time scale, implies that analysis tools must not integrate over time scales longer than the intermittent time scale; (2) non-linearity, a basic property of all numerical models of chaos and turbulence, requires specially adapted tools for its proper detection.

Recently, we have developed a statistically stable spectral analysis technique with time resolution based on wavelet analysis. We stress that statistical stability is an essential requirement for extracting meaningful information from turbulent phenomena.

We apply these techniques to the analysis of Langmuir probe data in the plasma edge region of the TJ-I U torsatron, in discharges with steady or modulated Electron Cyclotron Resonant Heating. We draw some tentative conclusions about radial correlation lengths.

1 Introduction

Although the phenomenon of turbulence is only partially understood, there seems to be consensus on several aspects. First, that *intermittence* is a basic property of turbulence. This means that the characteristics of the turbulence (spectral distribution, amplitude etc.) vary on a short time scale. Analysis techniques that rely on the accumulation of data over time scales larger than this characteristic time scale will then average out much of the dynamics and obliterate relevant information (as may occur with Fourier analyses).

Wavelet analysis is ideally suited to tackle this problem. Standard wavelet analysis is, however, not fully adequate since it is not statistically robust. In this paper we shall develop statistically stable wavelet techniques.

Second, it is generally accepted that turbulence only arises in *non-linear* systems. Therefore, to understand the nature of turbulence, it is essential to employ analysis tools that are capable of handling this non-linearity. The usual analyses based on (cross-) spectra and (cross-) correlations, essentially linear analysis techniques, are not adequate.

Non-linear analysis tools can be obtained by generalizing the common spectral analysis methods to higher order, which then are sensitive to non-linear interactions. We focus on the so-called bispectral analysis, a method for the detection of quadratic interactions. Statistical stability of the bispectrum – a third-order spectrum – is again an important point, and noise level estimates can be provided. The main application of the bispectrum is the detection of phase coupling. It has been shown in earlier publications [1, 2] how reasonable time resolution, relevant to intermittency in some turbulent phenomena, can be achieved. Also it has been discussed how the bicoherence is related to non-linearity and the presence of structure in turbulence.

2 Spectral analysis tools

In this section we give a statistically robust definition of the wavelet cross spectrum and cross coherence.

2.1 Wavelet analysis

In the present work we use the continuous wavelet transform based on the Morlet wavelet which has the benefit of conceptual closeness to the Fourier analysis base functions $e^{-i\omega t}$:

$$\Psi(t) = \pi^{-1/4} \exp\left[-i2\pi t - \frac{1}{2}t^2\right]; \quad \Psi_a(t) = a^{-1/2} \Psi(t/a) \quad (1)$$

We assign a frequency $\omega = 2\pi/a$ to each scale a . The frequency resolution of the wavelet $\Psi_a(t)$ is approximately $\Delta\omega = \omega/4$, and the time resolution is $\Delta t = 2a$. Note that $\Delta\omega \cdot \Delta t = \pi$, independent of a .

The wavelet transform of a function $f(t)$ is defined by [3, 4]:

$$W_f(a, \tau) = \int f(t) \Psi_a(t - \tau) dt \quad (2)$$

The advantage of the wavelet analysis lies in the fact that the time resolution is variable with frequency, so that high frequencies have a sharper time resolution. Thus, turbulent signals are decomposed into oscillations that die out in time, and more rapidly so with increasing frequency, which seems more natural for turbulence than the Fourier picture of stationary oscillations.

2.2 Statistically robust wavelet spectral analysis

In order to obtain statistical stability for our spectral analysis tools while maintaining time resolution, we average appropriate combinations of wavelet coefficients over a (small) finite time interval $T: \{T_0 - T/2 \leq \tau \leq T_0 + T/2\}$. This procedure allows the estimation of a noise level which will tell us the statistical significance of the obtained results.

Thus, for example, the wavelet cross spectrum is given by:

$$C_{fg}^w(a, T_0) = \int_T W_f^*(a, \tau) W_g(a, \tau) d\tau \quad (3)$$

where $f(t)$ and $g(t)$ are two time series and C_{fg}^w is complex. The normalized wavelet cross coherence is:

$$\gamma_{fg}^w(a, T_0) = \frac{\left| \int_T W_f^*(a, \tau) W_g(a, \tau) d\tau \right|}{\left(P_f^w(a, T_0) P_g^w(a, T_0) \right)^{1/2}} \quad (4)$$

which can take on values between 0 and 1. Here the wavelet auto-power spectrum is $P_f^w(a, T_0) = C_{ff}^w(a, T_0)$.

To calculate γ_{fg}^w (Eq. 4), the wavelet coefficients are determined for each of $N = T \cdot f_{\text{samp}}$ samples in the interval T and averaged (Eq. 2), where $\omega_{\text{samp}} = 2\pi f_{\text{samp}}$ is the sampling frequency. However, these wavelet coefficients are not all statistically independent, since the chosen wavelet family is not orthogonal. Due to the periodicity a of the wavelets, two statistically independent estimates of the wavelet coefficients are separated by a time $a/2$, or by a number of points $M(a) = a \cdot \omega_{\text{samp}} / 4\pi$. Thus, the integral appearing in Eq.(2) is carried out over $N/M(a)$ independent estimates of wavelet coefficients. Using this, we may estimate the statistical noise level as:

$$\varepsilon(\gamma_{fg}^w(a, T_0)) \approx 2 \left[\frac{\omega_{\text{samp}}}{\omega} \frac{1}{N} \right]^{1/2} \quad (5)$$

The value of γ_{fg}^w as obtained for Gaussian noise conforms quite well to this prediction.

Similar definitions can be given for higher-order spectra that measure the presence of non-linear interactions. Refer to Refs. [1, 2] for the corresponding definitions.

3 Radial coherence observed on the TJ-I U torsatron

In the following, we analyze discharges on the TJ-I U Torsatron with steady Electron Cyclotron Resonant Heating (ECRH) in Section 3.1, and with modulated ECRH in Section 3.2

3.1 Steady ECRH discharges

The time-resolved radial turbulent flux, $\Gamma_T = \tilde{n} \tilde{E}_\theta / B_T$, was measured at two radially separated positions (separation 1 cm) in the plasma edge region of the TJ-I U Torsatron [5]. The plasmas were heated by ECRH, and have $R = 0.6$ m, central rotational transform $i(0) = 0.21$, $\langle a \rangle = 0.1$ m, $B_t = 0.6$ T, and $n_e = 5 \times 10^{18} \text{ m}^{-3}$. Each of the two probes has three tips, aligned perpendicular to the magnetic field and separated poloidally by $\Delta = 0.2$ cm. The probes were designed and positioned to avoid shadowing effects [6, 7]. The fluctuating poloidal electric field

is then derived from the measured fluctuating floating potential in the two most extreme probe tips: $\tilde{E}_\theta = (\tilde{\Phi}_f(1) - \tilde{\Phi}_f(2))/\Delta$. The third probe tip is located between the other two, but slightly displaced toroidally. It is set up to measure the ion saturation current I_{sat} . The turbulent flux Γ_T has been calculated neglecting the influence of temperature fluctuations ($\tilde{n} \propto \tilde{I}_{sat}$). The signals are sampled at 1 MHz.

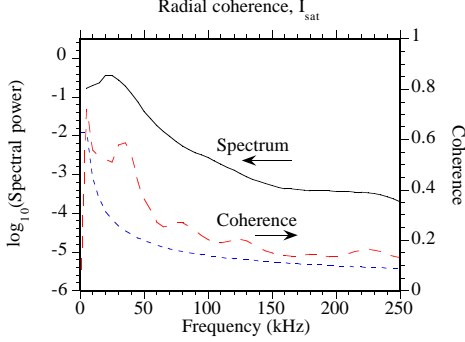


Fig. 1a Cross spectrum and cross coherence of I_{sat} from two radially separated probes in the edge zone of a TJ-I U plasma. Continuous line: average wavelet spectrum; long dashes: wavelet coherence; short dashes: the noise level of the coherence.

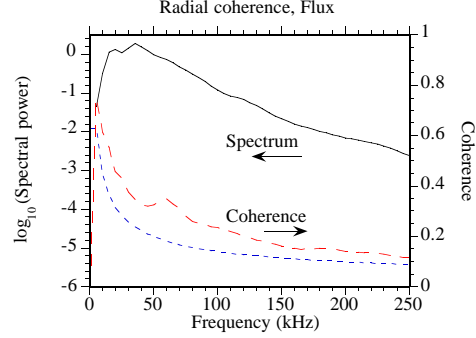


Fig. 1b Same as Fig. 1a for the instantaneous particle flux derived from the probe data (see text). The value of the coherence is smaller than for I_{sat} (Fig. 1a).

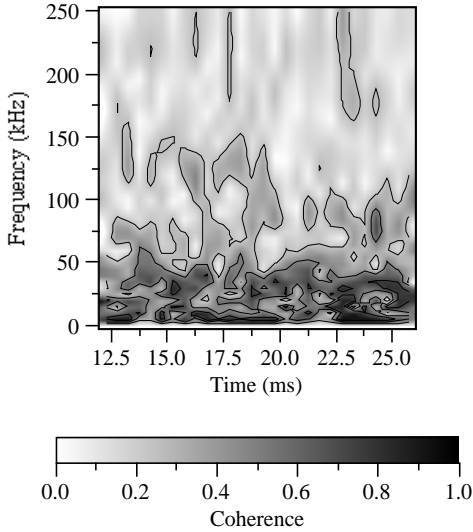


Fig. 2 Time-resolved wavelet coherence-versus-time graph of I_{sat} . The coherence is between two radially separated probes (see text). The noise level is the same as in Fig. 1. In several time intervals and at various frequencies the coherence obtains values far above the time-average value.

power was modulated with a modulation depth of 25% and an average input power of 200 kW. Power absorption is of the order of 30% according to ray-tracing calculations.

Fig. 3 shows the raw data of the floating point measurements at two radial positions. The effect of the modulation is clearly visible. Fig. 4 shows the time-average radial linear cross correlation for various signals. Notably, the cross correlation of the instantaneous flux is again significantly lower than the cross correlation of, e.g., I_{sat} .

Just as in the non-modulated ECRH discharges, the bicoherence between radially separated signals is generally low (close to noise level) for all signals, with the notable exception of the instantaneous flux in the time interval 6-12 ms. This is precisely the interval where the modulation of the raw signals is clearest (Fig. 3). As an example, Fig. 5 shows the

Fig. 1a shows the cross spectrum and radial cross-correlation between the \tilde{I}_{sat} signals of the two radially separated probes. Frequency scales were cut off at 250 kHz. The influence of a MHD mode is recognized in the peak of the spectrum at about 20 kHz. The cross correlation peaks at slightly higher frequency (35 kHz).

Fig. 1b shows the same graph, now calculated for Γ_T . Features similar to the ones observed in Fig. 1a can be seen, although at higher frequencies. This frequency shift is easily explained by the fact that Γ_T is a quadratic signal. What is most interesting is that the flux does not show a larger radial correlation than \tilde{I}_{sat} (or $\tilde{\Phi}_f$ either, not shown).

Fig. 2 shows the temporally resolved coherence of \tilde{I}_{sat} . The time resolution is 0.5 ms. The noise level is the same as in Fig. 1. The coherence is highly intermittent and occasionally very high values are achieved (much higher than the time-average value).

3.2 Modulated ECRH discharges

The discharges analyzed here are of the same type as those mentioned in the previous section. Here, ECRH

bicoherence and summed bicoherence, respectively, of the flux in the time interval 7-9 ms. The frequencies involved in the non-linear processes detected by the bicoherence do not appear to be related to the ECRH modulation frequency (1 kHz). It may be speculated that the modulation provides an indirect drive of some instabilities at higher frequencies. More investigation is needed to establish the nature of the instabilities and the driving mechanisms involved.

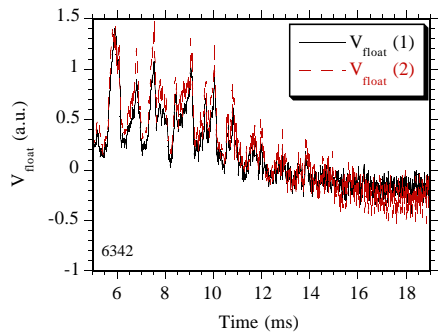


Fig. 3 Raw data of floating potential measurements at two radially separated positions in a discharge with ECRH modulation in TJ-I U.

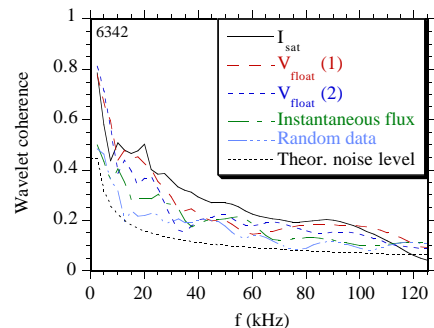


Fig. 4 Radial cross coherence between two radially separated probes. Radial coherence is highest for the saturation current, I_{sat} , while the floating potentials show similar coherence levels. Coherence is significantly lower for the instantaneous particle flux. For comparison, a curve is also shown for a similar analysis applied to random generated data; its coherence level is close to the theoretical noise level, as expected.

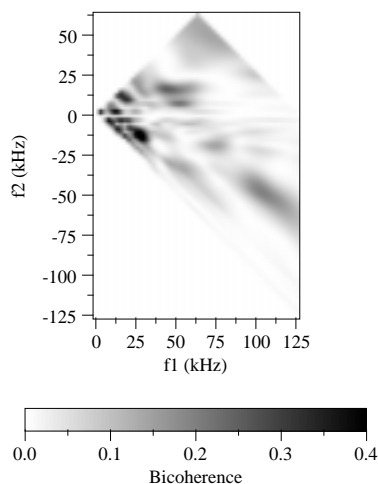


Fig. 5a Bicoherence of the instantaneous flux in the interval 7-9 ms

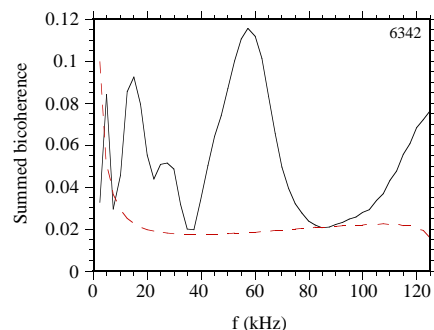


Fig. 5b Summed bicoherence of the instantaneous flux in the interval 7-9 ms.

References

- [1] B. Ph. van Milligen, C. Hidalgo and E. Sánchez, *Phys. Rev. Lett.* **74**, 3 (1995) 395
- [2] B.Ph. van Milligen, E. Sánchez, T. Estrada, C. Hidalgo, B. Brañas, B. Carreras, L. García, *Phys. Plasmas* **2** (8) (1995) 3017
- [3] C. Chui, *An introduction to wavelets*, Academic Press, New York (1992)
- [4] I. Daubechies, *Ten Lectures on Wavelets*, National Science Foundation Series In Applied Mathematics, S.I.A.M. (1992)
- [5] E. Ascasibar, C. Alejandre, J. Alonso, *et al.*, IAEA Conference, Seville, Spain, 1994, *Plasma Phys. and Contr. Nucl. Fusion Research*, IAEA-CN-60/A6-1, **1** (1994) 749
- [6] M.A. Pedrosa, C. Hidalgo, B. van Milligen, E. Sánchez, R. Balbín, I. García-Cortés, H. Niedermeyer, L. Giannone, *Proc. 23rd Eur. Conf. Kiev*, 1996
- [7] B.A. Carreras, C. Hidalgo, E. Sánchez, M.A. Pedrosa, R. Balbín, I. García-Cortés, B.Ph. van Milligen, D.E. Newman, V.E. Lynch, *Fluctuation-induced flux at the plasma edge in toroidal devices*, *Phys. Plasmas* **3** (7) (1996) 2664